International Journal for Uncertainty Quantification, 6 (5): 429–443 (2016)

A MULTIMODES MONTE CARLO FINITE ELEMENT METHOD FOR ELLIPTIC PARTIAL DIFFERENTIAL EQUATIONS WITH RANDOM COEFFICIENTS

Xiaobing Feng,[1] Junshan Lin,[2,] & Cody Lorton[3]*

[1] *Department of Mathematics, The University of Tennessee, Knoxville, Tennessee 37996, USA*

[2] *Department of Mathematics and Statistics, Auburn University, Auburn, Alabama 36849, USA*

[3] *Department of Mathematics and Statistics, University of West Florida, Pensacola, Floridas 32514, USA*

[*] Address all correspondence to: Junshan Lin, E-mail: jzl0097@auburn.edu

Original Manuscript Submitted: 3/22/2016; Final Draft Received: 10/5/2016

This paper develops and analyzes an efficient numerical method for solving elliptic partial differential equations, where the diffusion coefficients are random perturbations of deterministic diffusion coefficients. The method is based upon a multimodes representation of the solution as a power series of the perturbation parameter, and the Monte Carlo technique for sampling the probability space. One key feature of the proposed method is that the governing equations for all the expanded mode functions share the same deterministic diffusion coefficient; thus an efficient direct solver by repeatedly using the LU decomposition of the discretized common deterministic diffusion operator can be employed for solving the finite element discretized linear systems. It is shown that the computational complexity of the algorithm is comparable to that of solving a few deterministic elliptic partial differential equations using the director solver. Error estimates are derived for the method, and numerical experiments are provided to test the efficiency of the algorithm and validate the theoretical results.

KEY WORDS: *random partial differential equations, multimodes expansion, LU decomposition, Monte Carlo method, finite element methods*

1. INTRODUCTION

There has been increased interest in numerical approximation of random partial differential equations (PDEs) in recent years, due to the need to model the uncertainties or noises that arise in industrial and engineering applications [1–6]. To solve random boundary value problems numerically, the Monte Carlo method obtains a set of solutions by sampling the independent identically distributed (i.i.d.) PDE coefficients, and calculates the mean of the solution via a statistical average over all the samples in the probability space [3]. The stochastic Galerkin method, on the other hand, reduces the random PDE to a high-dimensional deterministic equation by expanding the random coefficients in the equation using the Karhunen-Loève (cf. [1, 2, 7–10]) or Wiener chaos expansions (cf. [6, 11, 12]). In general, these two methods become computationally expensive when a large number of degrees of freedom is involved in the spatial discretization, particularly for three-dimensional boundary value problems. The Monte Carlo method requires solving the boundary value problem many times with different sample coefficients, while the stochastic Galerkin method usually leads to a high-dimensional deterministic equation that may be too expensive to solve.

Recently, we have developed a new efficient multimodes Monte Carlo method for modeling acoustic wave propagation in weakly random media [13]. To solve the governing random Helmholtz equation, the solution is represented

2152–5080/16/$35.00

by a sum of mode functions, where each mode satisfies a Helmholtz equation with deterministic coefficients and a random source. The expectation of each mode function is then computed using a Monte Carlo interior penalty discontinuous Galerkin (MCIP-DG) method. We take the advantage that the deterministic Helmholtz operators for all the modes are identical, and employ an LU direct solver for obtaining the numerical solutions. Since the discretized equations for all the modes have the same constant coefficient matrix, by using the LU decomposition matrices repeatedly, the solutions for all samples of mode functions are obtained in an efficient way by performing simple forward and backward substitutions. This leads to a tremendous saving in the computational costs. Indeed, as discussed in [13], the computational complexity of the proposed algorithm is comparable to that of solving a few deterministic Helmholtz problems using the LU direct solver.

In this paper, we apply the multimodes Monte Carlo method for approximating the solution to the following random elliptic problem:

$$-\nabla \cdot (a(\omega,\cdot)\nabla u^{\varepsilon}(\omega,\cdot)) = f(\omega,\cdot) \qquad \text{in } D, \tag{1.1}$$

$$u^{\varepsilon}(\omega,\cdot) = 0 \qquad \text{on } \partial D. \tag{1.2}$$

Here D is a bounded Lipschitz domain in $\mathbb{R}^d$ ($d = 1,2,3$), and ω denotes the sample. $a(\omega,x)$ and $f(\omega,x)$ are random fields with continuous and bounded covariance functions. Let $(\Omega,\mathcal{F},P)$ be a probability space with sample space Ω, $\sigma-$algebra, $\mathcal{F}$ and probability measure P. We consider the case when the diffusion coefficient $a(\omega,x)$ in (1.1) is a small random perturbation of some deterministic diffusion coefficient, namely,

$$a(\omega,\cdot) := a_0(\cdot) + \varepsilon\eta(\omega,\cdot). \tag{1.3}$$

Here $a_0 \in W^{1,\infty}(D)$, ε represents the magnitude of the random fluctuation, and $\eta \in L^2(\Omega, W^{1,\infty}(D))$ is a random function satisfying

$$P\left\{\omega \in \Omega : \ ||\eta(\omega,\cdot)||_{W^{1,\infty}(D)} \le b_0\right\} = 1$$

for some positive constant b_0. The readers are referred to Section 2 for the definition of the function spaces $W^{1,\infty}(D)$ and $L^2(\Omega, W^{1,\infty}(D))$. The random diffusion coefficient (1.3) can be interpreted as diffusion through a random perturbation of some deterministic background medium. It is required that $a(\omega,x)$ is uniformly coercive. That is, there exists a positive constant $\underline{a}$ such that

$$P\left\{\omega \in \Omega : \min_{x\in\bar{D}} a(\omega,x)) > \underline{a}\right\} = 1.$$

The proposed numerical method is based on the following multimodes expansion of the solution:

$$u^{\varepsilon}(\omega,x) = \sum_{n=0}^{\infty} \varepsilon^n u_n(\omega,x).$$

It is shown in this paper that the series converges to u^{ε} and each mode u_n satisfies an elliptic equation with deterministic coefficients and a random source. We apply the Monte Carlo method for sampling over the probability space Ω and use the finite element method for solving the boundary value problem for u_n at each realization. An interesting and important fact of the mode expansion is that all u_n share the same deterministic elliptic operator $\nabla\cdot(a_0\nabla)$; hence the LU decomposition of the finite element stiffness matrix can be used repeatedly. As such, solving for $u_n(\omega,x)$ for each n and at each realization $\omega = \omega_j$ only involves simple forward and backward substitutions with the L and U matrices, and the computational complexity for the algorithm can be significantly reduced. It should be pointed out that here the randomly perturbed diffusion coefficient $a(\omega,x)$ appears in the leading term of the elliptic differential operator, while for the Helmholtz equation considered in [13], the random coefficient only appears in the low-order term. This results in the main differences in both computation and analysis when the multimodes expansion idea is applied to these two problems.

The rest of the paper is organized as follows. We begin with introducing some space notation in Section 2 and discuss the well-posedness of problems (1.1) and (1.2). In Section 3, we introduce the multimodes expansion of the

solution as a power series of ε, and derive the error estimation for its finite-modes approximation. The details of the multimodes Monte Carlo method are given in Section 4, where the computational complexity of the algorithm and the error estimations for the numerical solution are also obtained. Several numerical experiments are provided in Section 5 to demonstrate the efficiency of the method and to validate the theoretical results. We end the paper with a discussion on generalization of the proposed numerical method to more general random PDEs in Section 6.

2. PRELIMINARIES

Standard space notations will be adopted in this paper [14–16]. For example, $L^2(D)$ denotes the Hilbert space of all square integrable functions equipped with the inner product $(f,g)_D := \int_D fg\,dx$ and the induced norm

$$||u||_{L^2(D)} = \left(\int_D |u(x)|^2 dx\right)^{1/2},$$

and $L^\infty(D)$ is the set of bounded measurable functions equipped with the norm

$$||u||_{L^\infty(D)} = \operatorname*{esssup}_{x\in D}|u(x)|.$$

For a positive integer m and a fraction $s = m + \sigma$ with some $\sigma \in (0,1)$, we define the Sobolev spaces $H^m(D)$ and $H^s(D)$ as

$$H^m(D) := \{u \in L^2(D) :\ ||u||_{H^m(D)} < \infty\}, \tag{2.1}$$

$$H^s(D) := \{u \in L^2(D) :\ ||u||_{H^s(D)} < \infty\}, \tag{2.2}$$

where

$$||u||^2_{H^m(D)} := \sum_{|\alpha|\le m} ||\partial^\alpha u||^2_{L^2(D)},$$

$$||u||^2_{H^s(D)} := ||u||^2_{H^m(D)} + \sum_{|\alpha|=m} \int\int \frac{|\partial^\alpha u(x) - \partial^\alpha u(y)|^2}{|x-y|^{d+2\sigma}} dxdy.$$

We also define $H^m_0(D)$ and $H^s_0(D)$ to be the subspaces of $H^m(D)$ and $H^s(D)$ with zero trace, and $H^{-m}(D)$ and $H^{-s}(D)$ as the dual spaces of $H^m_0(D)$ and $H^s_0(D)$, respectively. The Sobolev space $W^{1,\infty}(D)$ is given by

$$W^{1,\infty}(D) := \{u \in L^\infty(D) :\ ||u||_{W^{1,\infty}(D)} < \infty\},$$

where $||u||_{W^{1,\infty}(D)} := ||u||_{L^\infty(D)} + ||\nabla u||_{L^\infty(D)}$. Finally, for a Banach space X, let $L^2(\Omega, X)$ denote the space of all measurable function $u : \Omega \to X$ such that

$$\|u\|_{L^2(\Omega,X)} := \left(\int_\Omega \|u(\omega,\cdot)\|^2_X dP(\omega)\right)^{1/2} < \infty.$$

Later in this paper, we shall take X to be $H^m(D)$, $H^s(D)$, or $W^{1,\infty}(D)$.

For a given source function $f \in L^2(\Omega, H^{-1}(D))$, a weak solution for problems (1.1) and (1.2) is defined as a function $u \in L^2(\Omega, H^1_0(D))$ such that

$$\int_\Omega \left(a\nabla u^\varepsilon, \nabla v\right)_D dP = \int_\Omega \langle f, v\rangle_D\, dP \qquad \forall v \in L^2(\Omega, H^1_0(D)), \tag{2.3}$$

where $(\cdot,\cdot)_D$ stands for the inner product on $L^2(D)$, and $\langle\cdot,\cdot\rangle_D$ denotes the dual product on $H^{-1}(D)\times H^1_0(D)$. Following the standard energy estimates and applying the Lax-Milgram theorem, it can be shown that (2.3) attains a

unique solution in $u \in L^2(\Omega, H_0^1(D))$ [2, 15, 16]. If $f \in L^2(\Omega, H^{-1+\sigma}(D))$ with $\sigma \in (0,1]$ and the boundary of the domain D is sufficiently smooth, then elliptic regularity theory gives rise to the following energy estimate (cf. [16]):

$$\mathbb{E}(\|u^\varepsilon\|^2_{H^{1+\sigma}(D)}) \le C\,\mathbb{E}(\|f\|^2_{H^{-1+\sigma}(D)}), \tag{2.4}$$

where $\mathbb{E}$ denotes the expected value, and C is some constant deepening on $a(\omega, x)$ and the domain D. In particular, when $\sigma = 1$, or equivalently $f \in L^2(\Omega, L^2(D))$, we have

$$\mathbb{E}(\|u^\varepsilon\|^2_{H^2(D)}) \le C\,\mathbb{E}(\|f\|^2_{L^2(D)}). \tag{2.5}$$

3. MULTIMODES EXPANSION OF THE SOLUTION

Our multimodes Monte Carlo method will be based on the following multimodes representation for the solution of problems (1.1) and (1.2):

$$u^\varepsilon(\omega, x) = \sum_{n=0}^{\infty} \varepsilon^n u_n(\omega, x), \tag{3.1}$$

where the convergence of the series will be justified below.

Substituting the above expansion into (1.1) and matching the coefficients of ε^n order terms for $n = 0, 1, 2, \cdots$, it follows that

$$-\nabla \cdot (a_0 \nabla u_0(\omega, \cdot)) = f(\omega, \cdot), \tag{3.2}$$

$$-\nabla \cdot (a_0 \nabla u_n(\omega, \cdot)) = \nabla \cdot (\eta \nabla u_{n-1}(\omega, \cdot)) \qquad \text{for } n \ge 1. \tag{3.3}$$

Correspondingly, the boundary condition for each mode function u_n is given by

$$u_n(\omega, \cdot) = 0 \qquad \text{on } \partial D \qquad \text{for } n \ge 0. \tag{3.4}$$

It is clear that each mode satisfies an elliptic equation with the same deterministic coefficient a_0 and a random source term. On the other hand, for $n \ge 1$, the source term in the PDE is given by the previous mode u_{n-1}. This implies that the mode u_n has to be solved recursively for $n = 0, 1, 2, \cdots$. We first derive the energy estimate for each mode u_n.

Theorem 3.1. *There exists a unique solution $u_n \in L^2(\Omega, H_0^1(D))$ to the problem* (3.2) *and* (3.4) *for $n = 0$, and the problem* (3.3)–(3.4) *for $n \ge 1$. In addition, if $f \in L^2(\Omega, H^{-1+\sigma}(D))$ for $\sigma \in (0,1]$, it holds that*

$$\mathbb{E}(\|u_n\|^2_{H^{1+\sigma}(D)}) \le C_0^{n+1}\,\mathbb{E}(\|f\|^2_{H^{-1+\sigma}(D)}), \tag{3.5}$$

for some constant C_0 independent of n and ε.

Proof. For $n = 0$, the existence of the weak solutions can be deduced from the Lax-Milgram theorem, and the desired energy estimate,

$$\mathbb{E}(\|u_0\|^2_{H^{1+\sigma}(D)}) \le \tilde{C}_0\,\mathbb{E}(\|f\|^2_{H^{-1+\sigma}(D)}),$$

follows directly by the elliptic regularity theory [16].

We show the case of $n \ge 1$ by induction. Assume that (3.5) holds for $n = 0, 1, \cdots, l-1$, then for the source term in (3.3), it follows that $\nabla \cdot (\eta \nabla u_{l-1}) \in L^2(\Omega, H^{-1+\sigma}(D))$. By the Lax-Milgram theorem, there exists $u_l \in L^2(\Omega, H_0^1(D))$ solving (3.3) for $n = l$. Let $C_0 = \tilde{C}_0 b_0^2$; by the elliptic regularity theory [16], we get

$$\begin{aligned}
\mathbb{E}(\|u_l\|^2_{H^{1+\sigma}(D)}) &\le \tilde{C}_0\,\mathbb{E}(\|\nabla \cdot (\eta \nabla u_{l-1})\|^2_{H^{-1+\sigma}(D)}) \\
&\le \tilde{C}_0 \left(\mathbb{E}(\|\nabla \eta \cdot \nabla u_{l-1})\|^2_{H^{-1+\sigma}(D)}) + \mathbb{E}(\|\eta \Delta u_{l-1}\|^2_{H^{-1+\sigma}(D)})\right) \\
&\le \tilde{C}_0 b_0^2\,\mathbb{E}(\|u_{l-1}\|^2_{H^{1+\sigma}(D)}) \\
&\le C_0^{l+1}\,\mathbb{E}(\|f\|^2_{H^{-1+\sigma}(D)}).
\end{aligned}$$

This completes the proof. □

A more practical and interesting mode expansion for the solution is given by its finite-terms approximation. Namely, for a non-negative integer N, we define the partial sum,

$$U_N^\varepsilon(\omega,x) := \sum_{n=0}^{N-1} \varepsilon^n u_n(\omega,x), \tag{3.6}$$

and the remainder,

$$r_N^\varepsilon(\omega,x) := u^\varepsilon(\omega,x) - U_N^\varepsilon(\omega,x). \tag{3.7}$$

For a given N, an upper bound for the remainder r_N^ε is established by the following theorem.

Theorem 3.2. *Assume that $\varepsilon < 1$ and $f \in L^2(\Omega, H^{-1+\sigma}(D))$ for $\sigma \in (0,1]$. Let r_N^ε be the remainder defined above. Then*

$$\mathbb{E}(\|r_N^\varepsilon\|^2_{H^{1+\sigma}(D)}) \le C_0^{N+1}\varepsilon^{2N}\ \mathbb{E}(\|f\|^2_{H^{-1+\sigma}(D)}) \tag{3.8}$$

for some positive constant C_0 independent of N and ε.

Proof. By a direct comparison, it is easy to check that $r_1^\varepsilon = u^\varepsilon - u_0$ satisfies

$$\begin{aligned} -\nabla\cdot(a_0(\omega,\cdot)\nabla r_1^\varepsilon(\omega,\cdot)) &= \varepsilon\ \nabla\cdot(\eta(\omega,\cdot)\nabla u^\varepsilon(\omega,\cdot)) && \text{in } D,\\ r_1^\varepsilon(\omega,\cdot) &= 0 && \text{on } \partial D. \end{aligned}$$

Therefore,

$$\begin{aligned} \mathbb{E}(\|r_1^\varepsilon\|^2_{H^{1+\sigma}(D)}) &\le \tilde{C}_0\ \varepsilon^2\ \mathbb{E}(\|\nabla\cdot(\eta\nabla u^\varepsilon)\|^2_{H^{-1+\sigma}(D)})\\ &\le \tilde{C}_0 b_0^2\ \varepsilon^2\ \mathbb{E}(\|u^\varepsilon\|^2_{H^{1+\sigma}(D)})\\ &\le C_0^2\ \varepsilon^2\ \mathbb{E}(\|f\|^2_{H^{-1+\sigma}(D)}), \end{aligned}$$

where $C_0 = \tilde{C}_0(1+b_0^2)$. Assume that (3.8) holds for $n = 1,\cdots,l-1$. For $n = l$, it can be shown that r_l^ε is the solution of

$$\begin{aligned} -\nabla\cdot(a_0(\omega,\cdot)\nabla r_l^\varepsilon(\omega,\cdot)) &= \varepsilon\ \nabla\cdot\big(\eta(\omega,\cdot)\nabla r_{l-1}^\varepsilon(\omega,\cdot)\big) && \text{in } D,\\ r_l^\varepsilon(\omega,\cdot) &= 0 && \text{on } \partial D. \end{aligned}$$

A parallel argument as above yields the desired estimate

$$\mathbb{E}(\|r_l^\varepsilon\|^2_{H^{1+\sigma}(D)}) \le C_0\varepsilon^2\ \mathbb{E}(\big\|r_{l-1}^\varepsilon\big\|^2_{H^{1+\sigma}(D)}) \le C_0^{l+1}\varepsilon^{2l}\ \mathbb{E}(\|f\|^2_{H^{-1+\sigma}(D)}).$$

The proof is complete. □

In particular, by letting $N\to\infty$, we obtain the convergence of the partial sum U_N^ε:

Corollary 3.3. *Let $r_{N,\varepsilon}$ be the remainder defined in* (3.7)*. If $\varepsilon < \min\{1, C_0^{-\frac{1}{2}}\}$, then $\mathbb{E}(\|r_N^\varepsilon\|^2_{H^{1+\sigma}(D)}) \to 0$ as $N\to\infty$.*

Corollary 3.3 shows that the expansion (3.1) is valid and the partial sum U_N^ε given by (3.6) converges to u_ε as $N\to\infty$, as long as ε is sufficiently small.

4. MULTI-MODES MONTE CARLO METHOD

4.1 Numerical Algorithm and Computational Complexity

We introduce the multimodes Monte Carlo method for approximating the solution of the problem (1.1) and (1.2). The method is based upon the multimodes representation (3.1) and its finite-terms approximation (3.6). For each mode u_n, the standard finite difference or finite element method may be applied to discretize the elliptic partial differential

equations (3.2) and (3.3), and the classical Monte Carlo method is employed for sampling the probability space and for computing the statistics of the numerical solution. Here, we introduce the algorithm wherein the finite element method is used for solving the elliptic PDEs.

Let M be a large positive integer which denotes the number of realizations for the Monte Carlo method. $\mathcal{T}_h$ stands for a quasi-uniform triangular (if $d = 2$) or tetrahedral (if $d = 3$) partition of D such that $\overline{D} = \bigcup_{K\in\mathcal{T}_h} \overline{K}$. Let $h := \max\{h_K : K \in \mathcal{T}_h\}$, wherein h_K is the diameter of $K \in \mathcal{T}_h$, and J be number of the degrees of freedom associated with the triangulation $\mathcal{T}_h$ in each direction. Let V_r^h be the standard finite element space defined by

$$V_r^h := \big\{v \in H_0^1(D) : \ v|_K \text{ is a polynomial of degree at most } r \text{ for each } K \in \mathcal{T}_h\big\}.$$

For each $j = 1, 2, \cdots, M$, we sample i.i.d. realizations of the source function $f(\omega_j, \cdot)$ and random medium coefficient $\eta(\omega_j, \cdot)$. The finite element solutions for the mode $u_n^h(\omega_j, \cdot)$ are obtained recursively as follows:

$$\big(a_0\nabla u_0^h(\omega_j,\cdot), \nabla v^h\big)_D = \langle f(\omega_j,\cdot), v^h\rangle_D \qquad \forall v^h \in V_r^h, \tag{4.1}$$

$$\big(a_0\nabla u_n^h(\omega_j,\cdot), \nabla v^h\big)_D = -\big(\eta(\omega_j,\cdot)\nabla u_{n-1}^h(\omega_j,\cdot), \nabla v^h\big)_D \qquad \forall v^h \in V_r^h, \tag{4.2}$$

for $n \geq 1$. An application of the Lax-Milgram theorem and an induction argument for the variational problems (4.1) and (4.2) yield the following energy estimates for the finite element solution $u_n^h(\omega_j, \cdot)$.

Theorem 4.1. *If $f \in L^2(\Omega, H^{-1+\sigma}(D))$ for $\sigma \in (0, 1]$, it holds that for $n \geq 0$,*

$$\mathbb{E}\big(\, \|u_n^h\|_{H^1(D)}^2\big) \leq C_0^{n+1}\, \mathbb{E}(\|f\|_{H^{-1+\sigma}(D)}^2) \tag{4.3}$$

for some constant C_0 independent of n and ε.

We then approximate the expectation $\mathbb{E}(u_n)$ of each mode u_n by the average $1/M \sum_{j=1}^M u_n^h(\omega_j, \cdot)$. Consequently, by virtue of (3.6), the algorithm yields a finite-modes approximation of $\mathbb{E}(u^\varepsilon)$ given by

$$\Psi_N^h = \frac{1}{M}\sum_{j=1}^{M}\sum_{n=0}^{N-1} \varepsilon^n u_n^h(\omega_j, \cdot). \tag{4.4}$$

Importantly, it is observed from (3.2) and (3.3) that all the modes share the same deterministic elliptic operator $-\nabla\cdot(a_0\nabla)$ and the bilinear forms in (4.1) and (4.2) are identical. Using this crucial fact, it turns out that an LU direct solver for the discretized equations (4.1) and (4.2) leads to a tremendous saving in the computational costs. More precisely, we first compute an LU decomposition for the associated matrix of the bilinear form $\big(a_0\nabla u_n^h(\omega_j,\cdot), \nabla v^h\big)_D$. The resulting lower and upper triangular matrices, L and U, are stored and used repeatedly to obtain the solutions for all modes and all samples by simple forward and backward substitutions. This speeds up the sampling tremendously, since in contrast to a complete linear solver with $O(J^{3d})$ computational complexity, only an $O(J^{2d})$ computational complexity is involved to calculate one single sample by the use of forward and backward substitutions. Here d denotes the spatial dimension of the domain D. The precise description of this procedure is given in the Algorithm 1.

Algorithm 1.

Inputs: $f, \eta, \varepsilon, h, M, N$.

Set $\Psi_N^h(\cdot) = 0$ (initializing).

For $j = 1, 2, \cdots, M$

Set $U_N^h(\omega_j, \cdot) = 0$ (initializing).

Solve for $u_0^h(\omega_j, \cdot)$ by LU decomposition

$$\big(a_0\nabla u_0^h(\omega_j,\cdot), \nabla v^h\big)_D = \langle f(\omega_j,\cdot), v^h\rangle_D \quad \forall v_h \in V_r^h.$$

Set $U_N^h(\omega_j,\cdot) \leftarrow U_N^h(\omega_j,\cdot) + u_0^h(\omega_j,\cdot)$.
For $n = 1, \cdots, N-1$
Solve for $u_n^h(\omega_j,\cdot) \in V_r^h$ by LU decomposition

$$\big(a_0 \nabla u_n^h(\omega_j,\cdot), \nabla v^h\big)_D = -\big(\eta(\omega_j,\cdot)\nabla u_{n-1}^h(\omega_j,\cdot), \nabla v^h\big)_D,\ \forall v_h \in V_r^h.$$

Set $U_N^h(\omega_j,\cdot) \leftarrow U_N^h(\omega_j,\cdot) + \varepsilon^n u_n^h(\omega_j,\cdot)$.
End For
Set $\Psi_N^h(\cdot) \leftarrow \Psi_N^h(\cdot) + \frac{1}{M} U_N^h(\omega_j,\cdot)$.
End For

Output $\Psi_N^h(\cdot)$.

Remark 4.2. *We note that, instead of applying the standard Monte Carlo method for sampling over the probability space in the above algorithm, more efficient sampling techniques such as quasi Monte Carlo methods can be employed. The only difference lies in how ω_j is chosen in the outer loop of the algorithm [3]. It is also expected that the convergence rate of the numerical algorithm will be improved, due to the higher order convergence rate for the quasi Monte Carlo methods.*

Remark 4.3. *It is clear that the sample variance can also be computed by the using formula $1/M \sum_{j=1}^{M} (U_N^h(\omega_j,\cdot) - \Psi_N^h)^2$ in the above algorithm. No further computational cost is required.*

The algorithm requires to solve a total of MN linear systems for N modes and M realizations for each mode. Since all linear systems share the same coefficient matrix, we only need to perform one LU decomposition of the matrix and save the lower and upper triangular matrices. The decomposition is then reused to solve the remaining $MN-1$ linear systems by performing $MN-1$ sets of forward and backward substitutions. It is straightforward that the computational cost of the algorithm is $O[(2/3)J^{3d}] + O(MNJ^{2d})$. In light of Theorem 3.2, a relatively small number N of modes is needed to get the desired accuracy in practice, since the associated remainder r_N^ε has an order of ε^N. Hence we may regard N as a constant. To get the same order of errors for the finite element approximation and the Monte Carlo simulation (see Sections 4.2 and 5), we may choose $M \sim O(J^4)$. Consequently, the total cost for executing the algorithm becomes $O[2/3J^{3d}] + O(NJ^{2d+4})$. As a comparison, a brute force Monte Carlo method for solving the problems (1.1) and (1.2) with the same number of realization gives rise to $O[(2/3)J^{3d+4}]$ multiplications/divisions. It is clear that the computational cost of the proposed algorithm is significantly reduced by effectively using the LU director solver.

4.2 Convergence Analysis

In this subsection, we derive the error estimates for the proposed algorithm. First, it is observed that $\mathbb{E}(u^\varepsilon) - \Psi_N^h$ can be decomposed as

$$\mathbb{E}(u^\varepsilon) - \Psi_N^h = \big(\mathbb{E}(u^\varepsilon) - \mathbb{E}(U_N^\varepsilon)\big) + \big(\mathbb{E}(U_N^\varepsilon) - \mathbb{E}(U_N^h)\big) + \big(\mathbb{E}(U_N^h) - \Psi_N^h\big), \tag{4.5}$$

where U_N^ε and Ψ_N^h are given by (3.6) and (4.4), respectively, and

$$U_N^h(\omega,x) := \sum_{n=0}^{N-1} \varepsilon^n u_n^h(\omega,x).$$

It is clear that the first term in the decomposition (4.5) measures the error due to the finite-modes expansion, the second term is the spatial discretization error, and the third term represents the statistical error due to the Monte Carlo method.

The finite-modes representation error is given in Theorem 3.2. That is,

$$\mathbb{E}\big(\,\|u^\varepsilon - U_N^\varepsilon\|^2_{H^{1+\sigma}(D)}\big) \le C_0^{N+1}\varepsilon^{2N}\,\mathbb{E}\big(\,\|f\|^2_{H^{-1+\sigma}(D)}\big). \tag{4.6}$$

Let $\Phi_n^h = 1/M\sum_{j=1}^M u_n^h(\omega_j,\cdot)$; then it is clear that

$$\mathbb{E}(U_N^h) - \Psi_N^h = \sum_{n=0}^{N-1}\varepsilon^n\big(\mathbb{E}(u_n^h) - \Phi_n^h\big).$$

With the standard error estimates for the Monte Carlo method (cf. [2, 10]), the statistical error can be bounded as follows:

$$\begin{aligned}\mathbb{E}\big(\big\|\mathbb{E}(U_N^h) - \Psi_N^h\big\|^2_{H^1(D)}\big) &\le 2\sum_{n=0}^{N-1}\varepsilon^{2n}\,\mathbb{E}\big(\|\mathbb{E}(u_n^h) - \Phi_n^h\|^2_{H^1(D)}\big)\\ &\le \frac{2}{M}\sum_{n=0}^{N-1}\varepsilon^{2n}\,\mathbb{E}\big(\,\big\|u_n^h\big\|^2_{H^1(D)}\big).\end{aligned}$$

From Theorem 4.1, by choosing $\varepsilon \le \min\big\{1, 1/\sqrt{C_0}\big\}$, we have

$$\begin{aligned}\mathbb{E}\big(\big\|\mathbb{E}(U_N^h) - \Psi_N^h\big\|^2_{H^1(D)}\big) &\le \frac{2C_0}{M}\left(\sum_{n=0}^{N-1}\varepsilon^{2n}C_0^n\right)\mathbb{E}\big(\,\|f\|^2_{H^{-1+\sigma}(D)}\big)\\ &\le \frac{2C_0}{(1-C_0\varepsilon^2)M}\,\mathbb{E}\big(\,\|f\|^2_{H^{-1+\sigma}(D)}\big).\end{aligned} \tag{4.7}$$

In order to estimate the spatial discretization error $\mathbb{E}(U_N^\varepsilon) - \mathbb{E}(U_N^h)$, for each mode, let us define an auxiliary function $\tilde{u}_n^h \in V_r^h$ as the solution of the following discrete problem:

$$\big(a_0\nabla\tilde{u}_n^h(\omega_j,\cdot),\nabla v^h\big)_D = -\big(\eta(\omega_j,\cdot)\nabla u_{n-1}(\omega_j,\cdot),\nabla v^h\big)_D, \tag{4.8}$$

for all $v_h \in V_r^h$ and $n \ge 1$. For simplicity, we restrict ourselves to the case of $r = 1$. Namely, v^h is a linear polynomial on each $K \in \mathcal{T}_h$. The case of $r > 1$ can be derived similarly, and we omit it for the clarity of the exposition. The standard error estimation technique for the finite element method (cf. [17]) and the energy estimate (3.5) yield

$$\begin{aligned}\mathbb{E}\big(\big\|u_n - \tilde{u}_n^h\big\|_{H^1(D)}\big) &\le Ch^\sigma\,\mathbb{E}\big(\|u_n\|_{H^{1+\sigma}(D)}\big)\\ &\le C\big(\sqrt{C_0}\big)^{n+1}h^\sigma\,\mathbb{E}\big(\|f\|_{H^{-1+\sigma}(D)}\big).\end{aligned} \tag{4.9}$$

Next we estimate the error $\mathbb{E}\big(\big\|\tilde{u}_n^h - u_n^h\big\|_{H^1(D)}\big)$.

Recall that for $n \ge 1$, $u_n^h \in V_r^h$ is defined by

$$\big(a_0\nabla u_n^h(\omega_j,\cdot),\nabla v^h\big)_D = -\big(\eta(\omega_j,\cdot)\nabla u_{n-1}^h(\omega_j,\cdot),\nabla v^h\big)_D \quad \forall v_h \in V_r^h. \tag{4.10}$$

For each fixed sample $w = w_j$, a direct comparison of (4.8) and (4.10) gives rise to

$$\big(a_0(\nabla\tilde{u}_n^h - \nabla u_n^h),\nabla v^h\big)_D = -\big(\eta(\nabla u_{n-1} - \nabla u_{n-1}^h),\nabla v^h\big)_D \quad \forall v_h \in V_r^h.$$

By setting $v_h = \tilde{u}_n^h - u_n^h$ and using the Cauchy-Schwarz inequality, it follows that

$$\begin{aligned}\underline{a_0}\,\big\|\nabla\tilde{u}_n^h - \nabla u_n^h\big\|^2_{L^2(D)} &\le \big(a_0(\nabla\tilde{u}_n^h - \nabla u_n^h),\nabla\tilde{u}_n^h - \nabla u_n^h\big)_D\\ &= \big|\big(\eta(\nabla u_{n-1} - \nabla u_{n-1}^h),\nabla\tilde{u}_n^h - \nabla u_n^h\big)_D\big|\\ &\le b_0\,\big\|\nabla u_{n-1} - \nabla u_{n-1}^h\big\|_{L^2(D)}\,\big\|\nabla\tilde{u}_n^h - \nabla u_n^h\big\|_{L^2(D)},\end{aligned}$$

where $\underline{a_0} = \min_{x\in\bar{D}} a_0(x)$. We deduce that

$$\mathbb{E}\big(\|\nabla\tilde{u}_n^h - \nabla u_n^h\|_{L^2(D)}\big) \le b_0/\underline{a_0}\ \mathbb{E}\big(\|\nabla u_{n-1} - \nabla u_{n-1}^h\|_{L^2(D)}\big), \tag{4.11}$$

and an application of the Poincaré-Friedrichs inequality leads to the estimates

$$\mathbb{E}\big(\|\tilde{u}_n^h - u_n^h\|_{H^1(D)}\big) \quad \le \quad \beta\ \mathbb{E}\big(\|\nabla u_{n-1} - \nabla u_{n-1}^h\|_{L^2(D)}\big). \tag{4.12}$$

Here β is some constant depending on $\underline{a_0}$, b_0 and the domain D only.

In light of (4.9) and (4.12), we see that

$$\begin{aligned}\mathbb{E}\big(\|u_n - u_n^h\|_{H^1(D)}\big) &\le C\big(\sqrt{C_0}\big)^{n+1}h^\sigma\ \mathbb{E}\big(\|f\|_{H^{-1+\sigma}(D)}\big) + \beta\ \mathbb{E}\big(\|\nabla u_{n-1} - \nabla u_{n-1}^h\|_{L^2(D)}\big)\\ &\le C\big(\sqrt{C_0}\big)^{n+1}h^\sigma\ \mathbb{E}\big(\|f\|_{H^{-1+\sigma}(D)}\big) + \beta\ \mathbb{E}\big(\|u_{n-1} - u_{n-1}^h\|_{H^1(D)}\big).\end{aligned}$$

By applying the above inequality recursively, it is obtained that

$$\begin{aligned}\mathbb{E}\big(\|u_n - u_n^h\|_{H^1(D)}\big) \le Ch^\sigma\ \mathbb{E}\big(\|f\|_{H^{-1+\sigma}(D)}\big)\sum_{j=0}^{n-1}\beta^j\big(\sqrt{C_0}\big)^{n+1-j}\\ + \beta^n\ \mathbb{E}\big(\|u_0 - u_0^h\|_{H^1(D)}\big).\end{aligned} \tag{4.13}$$

Note that u_0 and u_0^h solve (3.2) and (4.1), respectively; hence

$$\mathbb{E}\big(\|u_0 - u_0^h\|_{H^1(D)}\big) \le Ch^\sigma\ \mathbb{E}\big(\|u_0\|_{H^{1+\sigma}(D)}\big) \le C\sqrt{C_0}h^\sigma\ \mathbb{E}\big(\|f\|_{H^{-1+\sigma}(D)}\big). \tag{4.14}$$

We arrive at

$$\mathbb{E}\big(\|u_n - u_n^h\|_{H^1(D)}\big) \le Ch^\sigma\ \mathbb{E}\big(\|f\|_{H^{-1+\sigma}(D)}\big)\sum_{j=0}^{n}\beta^j\big(\sqrt{C_0}\big)^{n+1-j} \tag{4.15}$$

by substituting (4.14) into (4.13). Correspondingly,

$$\begin{aligned}\mathbb{E}\big(\|U_N^\varepsilon - U_N^h\|_{H^1(D)}\big) &\le Ch^\sigma\ \mathbb{E}\big(\|f\|_{H^{-1+\sigma}(D)}\big)\sum_{n=0}^{N-1}\sum_{j=0}^{n}\varepsilon^n\beta^j\big(\sqrt{C_0}\big)^{n+1-j}\\ &\le C_1(\varepsilon,N)\ h^\sigma\ \mathbb{E}\big(\|f\|_{H^{-1+\sigma}(D)}\big),\end{aligned} \tag{4.16}$$

where

$$C_1(\varepsilon,N) := \frac{C\sqrt{C_0}}{\sqrt{C_0}-\beta}\left[\sqrt{C_0}\frac{1-(\varepsilon\sqrt{C_0})^N}{1-\varepsilon\sqrt{C_0}} - \beta\frac{1-(\varepsilon\beta)^N}{1-\varepsilon\beta}\right].$$

Combining (4.6), (4.7), and (4.16), we get the following error estimate for the full algorithm.

Theorem 4.4. *For a given source function $f \in L^2(\Omega, H^{-1+\sigma}(D))$ with $\sigma \in (0,1]$, let Ψ_N^h be the numerical solution obtained in the Main Algorithm with $r = 1$. It holds that*

$$\mathbb{E}\big(\|\mathbb{E}(u^\varepsilon) - \Psi_N^h\|_{H^1(D)}\big) \le C(\varepsilon^N + h^\sigma + M^{-1/2})\ \mathbb{E}\big(\|f\|_{H^{-1+\sigma}(D)}\big).$$

for some positive constant C independent of ε, h, M, and N.

Remark 4.5. *For the L^2-norm error $\mathbb{E}\big(\|\mathbb{E}(u^\varepsilon) - \Psi_N^h\|_{L^2(D)}\big)$ of the algorithm, it is expected that an order of $O\left(\varepsilon^N + h^{1+\sigma} + M^{-1/2}\right)$ can be achieved, as predicted by the numerical results in Section 5 (see Table 2).*

5. NUMERICAL EXPERIMENTS

In this section, we present a series of numerical experiments to illustrate the accuracy and efficiency of the proposed method. Section 5.1 studies the accuracy of the method for solving one-dimensional problems, where the analytical solution is known and hence can be used for comparison. The application of the numerical algorithm to two-dimensional problems is elaborated in Section 5.2. The linear finite element method is used to discretize the PDE; namely, we set $r = 1$, hence, u_h is a linear function on each $K \in \mathcal{T}_h$.

5.1 One-Dimensional Examples

We consider the following boundary value problem:

$$-\frac{d}{dx}\left(\big(1+\varepsilon Y(\omega)\big)\frac{du^\varepsilon(\omega,x)}{dx}\right) = Y(\omega), \qquad 0<x<1,$$
$$u^\varepsilon(\omega,0)=0, \quad u^\varepsilon(\omega,1)=0,$$

where $Y(\omega)$ is a uniformly distributed random variable over $[0,1]$. The analytical solution for the boundary value problem takes the form

$$u^\varepsilon(x,\omega) = \frac{Y(\omega)}{2(1+\varepsilon Y(\omega))}(x-x^2),$$

and its expectation is

$$\mathbb{E}(u^\varepsilon) = \frac{1}{2}\left(\frac{1}{\varepsilon}-\frac{1}{\varepsilon^2}\ln(1+\varepsilon)\right)(x-x^2).$$

To test the validity of the multimodes expansion and the accuracy of the numerical algorithm, we set $h = 0.01$ for the spatial discretization and $M = 10^6$ for the number of realizations. Table 1 displays the accuracy of the approximation for various ε and different number of modes, where the relative L^2-norm is defined as $\|\mathbb{E}(u^\varepsilon) - \Psi_N^h\|_{L^2(D)}/\|\mathbb{E}(u^\varepsilon)\|_{L^2(D)}$. It is observed that the multimodes Monte Carlo finite element method gives rise to accurate approximation as long as the magnitude of the random perturbation is not large. As expected, more modes are required to suppress the errors as the magnitude of the perturbation ε increases.

Next we study the convergence rate of the proposed algorithm numerically. Note that the global error consists of three parts as given in (4.5). The statistical error term arising from the Monte Carlo method is standard and we omit it here. In order to test the error term associated with the spatial discretization, we use large numbers of Monte Carlo realizations and adopt high-order mode expansion such that the total error of the algorithm is dominated by the spatial discretization error. To this end, we fix $\varepsilon = 0.5$ in the following and set $N = 10$, $M = 10^6$, respectively. The H^1 and L^2-norm errors for the multimodes Monte Carlo finite-element approximation Ψ_N^h are shown in Table 2. It is observed that a convergence rate of $O(h)$ is obtained for the numerical solution with respect to the H^1-norm. Note that $f \in L^2(\Omega, L^2(D))$ in this example; hence the numerical convergence rate is consistent with the theoretical one as obtained in Theorem 4.4. Furthermore, it is seen that the L^2-norm error exhibits a convergence rate of $O(h^2)$.

To study the convergence rate for the finite modes expansion, we fix $\varepsilon = 0.5$ and set $h = 0.01$, $M = 10^6$, respectively. For $N \le 4$, the error due to truncation of modes becomes dominant. Figure 1 displays the relative H^1-norm error for different modes. As expected, as the number of modes increases, the multimodes Monte Carlo finite

TABLE 1: Relative L^2-norm error for the multimodes Monte Carlo finite element approximation Ψ_N^h with different ε and N

ε	$N=2$	$N=3$	$N=4$	$N=5$	$N=6$
0.2	1.95×10^{-2}	3.15×10^{-3}	4.74×10^{-4}	1.45×10^{-4}	6.40×10^{-5}
0.4	7.66×10^{-2}	2.42×10^{-2}	8.05×10^{-3}	2.71×10^{-3}	9.84×10^{-4}
0.6	0.1688	0.0806	0.0391	0.0208	0.0100
0.8	0.2960	0.1869	0.1222	0.0839	0.0574

TABLE 2: H^1 and L^2-norm errors for the multimodes Monte Carlo finite element approximation Ψ_N^h with decreasing h, and the corresponding numerical convergence orders

h	$\|\mathbb{E}(u^\varepsilon) - \Psi_N^h\|_{H^1(D)}$	order	$\|\mathbb{E}(u^\varepsilon) - \Psi_N^h\|_{L^2(D)}$	order
0.2	2.19×10^{-1}		1.38×10^{-3}	
0.1	1.09×10^{-2}	1.00	3.29×10^{-4}	2.07
0.05	5.46×10^{-3}	1.00	7.43×10^{-5}	2.15
0.025	2.73×10^{-3}	1.00	1.28×10^{-5}	2.53

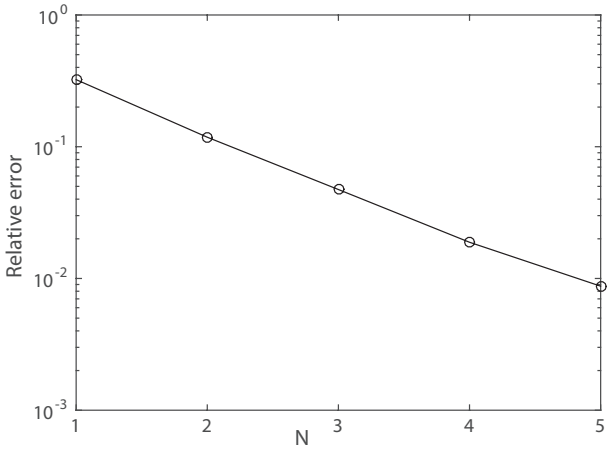

FIG. 1: Relative H^1-norm error for the multimodes Monte Carlo finite element approximation Ψ_N^h when different number of modes is used; $\varepsilon = 0.5$.

element approximation Ψ_N^h becomes more accurate and a convergence rate of $O(\varepsilon^N)$ is observed. This is consistent with the theoretical error estimation in Theorem 4.4.

5.2 Two-Dimensional Examples

We consider solving the two-dimensional random elliptic problem:

$$\begin{aligned} -\nabla \cdot \big(a(\omega,\cdot)\nabla u^\varepsilon(\omega,\cdot)\big) &= f(\omega,\cdot) \qquad \text{in } D, \\ u^\varepsilon(\omega,\cdot) &= 0 \qquad \text{on } \partial D, \end{aligned}$$

where the spatial domain is $D = (0,2)\times(0,2)$. The background diffusion coefficient $a_0(x_1,x_2) = 1$. The random perturbation $\eta(\omega,x)$ and the source function $f(\omega,x)$ are given by

$$\eta(\omega,x) = 0.5 + 0.5\sum_{m=1}^{M_\eta}\sum_{n=1}^{N_\eta} e^{-0.2(m^2+n^2)}\phi_{m,n}(x_1,x_2)Y_{m,n}(\omega),$$

$$f(\omega,x) = x_1^2 + x_2^2 + \sum_{m=1}^{M_f}\sum_{n=1}^{N_f} 2e^{-0.2(m^2+n^2)}\psi_{m,n}(x_1,x_2)Z_{m,n}(\omega),$$

respectively. Here $Y_{1,1}, \cdots, Y_{M_\eta,N_\eta}$ are independent uniformly distributed random variables over $[-1,1]$, and $Z_{1,1}, \cdots, Z_{M_f,N_f}$ are independent normally distributed random variables with mean 0 and variance 1. The basis functions are given by

$$\phi_{m,n}(x_1, x_2) = \cos(m\pi(x_1 - 1)) \cos(n\pi(x_2 - 1)),$$
$$\psi_{m,n}(x_1, x_2) = \sin(m\pi(x_1 - 1)) \sin(n\pi(x_2 - 1)).$$

We set $M_\eta = N_\eta = 10$, and $M_f = N_f = 5$ in the following numerical tests. From a simple calculation, it can be shown that $-0.6 \leq \eta \leq 1.6$ for the specified parameters.

To partition D, we use a quasi-uniform triangulation $\mathcal{T}_h$ with size h. The number of realizations for the Monte Carlo method is set as $M = 10{,}000$. As a benchmark, we compare the multimodes Monte Carlo method to the classical Monte Carlo finite element method (i.e., without utilizing the multimodes expansion). Let us denote the numerical approximation to $\mathbb{E}(u)$ using the classical Monte Carlo method by $\tilde{\Psi}^h$.

In order to test the efficiency of the multimodes Monte Carlo method, we set $h = 0.2$ and compare the CPU time for computing Ψ_N^h and $\tilde{\Psi}^h$. Both methods are implemented sequentially in Matlab on a Dell T7600 workstation. The results of this test are shown in Table 3. We find that the use of the multimodes expansion improves the CPU time for the computation considerably. In fact, the table shows that this improvement is an order of magnitude. Also, as expected, as the number of modes used is increased the CPU time increases in a linear fashion.

To give an illustration of computed solutions, we show the sample average Ψ_N^h and one computed sample U_N^h for $\varepsilon = 0.5$ and $\varepsilon = 0.8$ in Figs. 2 and 3, respectively. Here $N = 5$ is used for the multimodes expansion and $h = 0.05$ is set for the spatial discretization.

Next, we test the accuracy of the multimodes Monte Carlo finite-element approximation by using the standard Monte Carlo approximation $\tilde{\Psi}^h$ as the reference. To this end, the relative L^2-norm errors $\|\Psi_N^h - \tilde{\Psi}^h\|_{L^2(D)} / \|\tilde{\Psi}^h\|_{L^2(D)}$ are computed for various ε and different numbers of modes N. For clarity, we fix $h = 0.05$ for the spatial triangulation in this test. If $\varepsilon = 0.5$ is fixed, then the relative L^2-norm errors for different modes are shown in Fig. 4. Similar to the one-dimensional case, it is seen that as N increases, the difference between Ψ_N^h and $\tilde{\Psi}^h$ decreases steadily, and a rate of $O(\varepsilon^N)$ for the error is also observed. Moreover, if the number of modes used in the expansion is fixed as $N = 3$, the L^2-norm relative errors for ε ranges from 0.1 to 0.9 are plotted in Fig. 5. We see that even with three modes, the

TABLE 3: CPU time required to compute the classical Monte Carlo finite-element approximation $\tilde{\Psi}^h$ and the multimodes Monte Carlo finite-element approximation Ψ_N^h

Approximation	CPU Time (s)
$\tilde{\Psi}^h$	3.8077×10^5
Ψ_2^h	1.000×10^4
Ψ_3^h	1.313×10^4
Ψ_4^h	1.624×10^4
Ψ_5^h	1.957×10^4

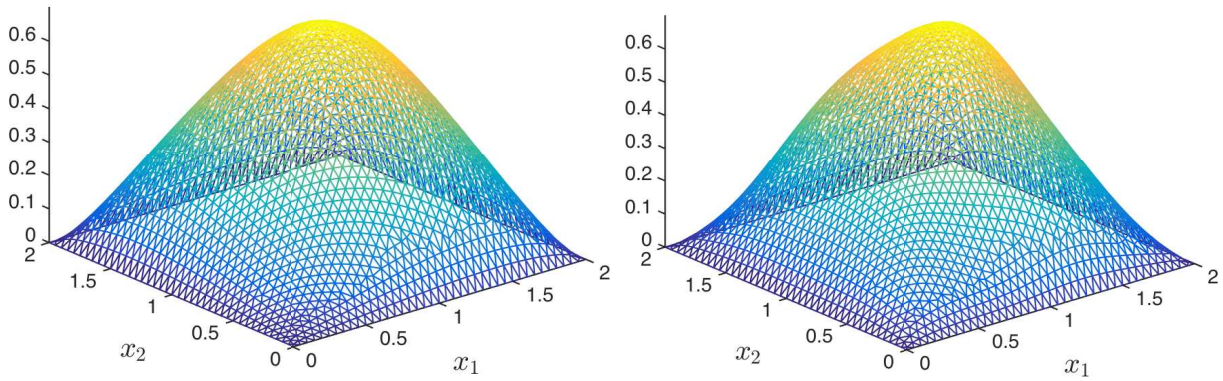

FIG. 2: The sample average Ψ_5^h (left) and one sample U_5^h (right) computed for $\varepsilon = 0.5$, and $M = 1000$.

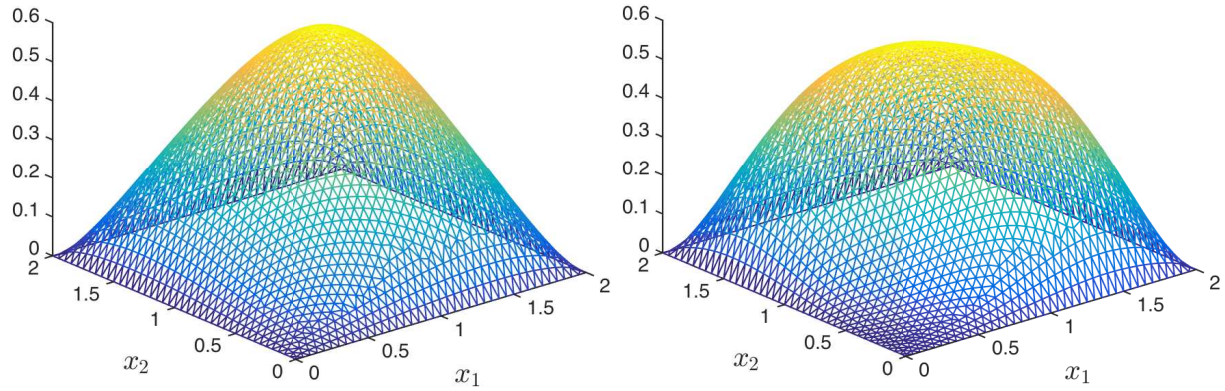

FIG. 3: The sample average Ψ_5^h (left) and one sample U_5^h (right) computed for $\varepsilon = 0.8$, and $M = 1000$.

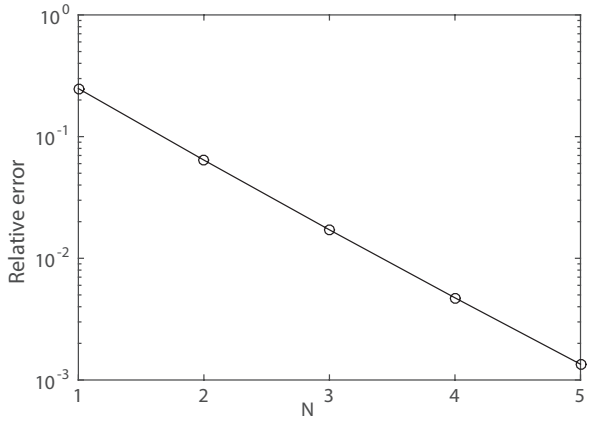

FIG. 4: Relative L^2-norm error between Ψ_N^h and $\tilde{\Psi}^h$ when different number of modes is used; $\varepsilon = 0.5$.

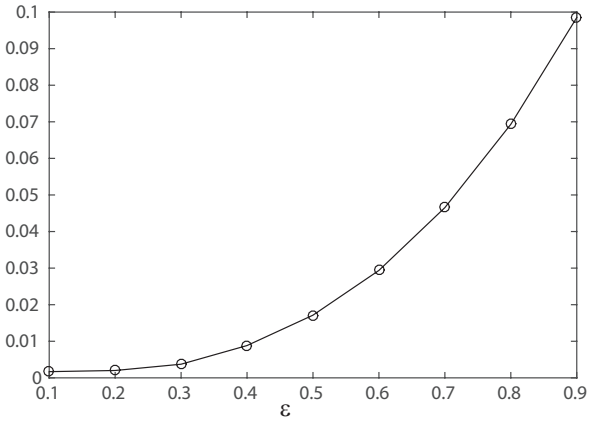

FIG. 5: Relative L^2-norm error between Ψ_N^h and $\tilde{\Psi}^h$ as ε increases. $N = 3$ is fixed for the multimodes Monte Carlo finite-element method.

multimodes Monte Carlo finite-element method already yields accurate approximation as long as the magnitude of the random perturbation is not large. As expected, more modes are required in the expansion to obtain more accurate solutions as ε increases. This is confirmed in Table 4, where the accuracy of the approximation for various ε and N

TABLE 4: Relative L^2-norm error between the multimodes Monte Carlo finite-element approximation Ψ_N^h and the classical Monte Carlo finite-element approximation $\tilde{\Psi}^h$ for different ε and N

ε	$N=2$	$N=3$	$N=4$	$N=5$
0.2	0.0104	0.0020	0.0016	0.0016
0.4	0.0416	0.0088	0.0026	0.0016
0.6	0.0923	0.0294	0.0101	0.0036
0.8	0.1632	0.0693	0.0309	0.0138

are displayed. It is noted that the accuracy for the case of $\varepsilon = 0.2$ does not get improved as N increases from 4 to 5. This is due to the fact that the total error of the algorithm is dominated by the error of spatial discretization when $N = 5$.

6. GENERALIZATION OF THE ALGORITHM TO GENERAL MEDIA

To use the multimodes Monte Carlo finite element method we developed above, it requires that the random media are weak in the sense that the leading coefficient a in the PDE has the form $a(\omega, x) = a_0(x) + \varepsilon\eta(\omega, x)$ and ε is not large. For more general random elliptic PDEs, their leading coefficients may not have the required "weak form." A natural question is whether the above multimodes Monte Carlo finite-element method can be extended to cover these random PDEs in which the diffusion coefficient $a(\omega, x)$ does not have the required form. A short answer to this question is yes. The main idea for overcoming this difficulty is first to rewrite $a(x, \omega)$ into the desired form $a_0(x) + \varepsilon\eta(\omega, x)$, then to apply the above "weak" field framework. There are at least two ways to do such a rewriting; the first one is to utilize the well-known Karhunen-Loève expansion and the second is to use a recently developed stochastic homogenization theory [18]. Since the second approach is more involved and lengthy to describe, below we only outline the first approach.

In many scenarios of geoscience and material science, the random media can be described by a Gaussian random field [4, 5, 19]. Let $\overline{a}(x)$ and $C(x, y)$ denote the mean and covariance function of the Gaussian random field $a(\omega, x)$, respectively. Two widely used covariance functions in geoscience and materials science are $C(x, y) = \exp(-|x - y|^m/\ell)$ for $m = 1, 2$ and $0 < \ell < 1$ (cf. Chapter 7 of [19]). Here ℓ is often called the correlation length which determines the range (or frequency) of the noise. The well-known Karhunen-Loève expansion for $a(\omega, x)$ takes the following form (cf. [19]):

$$a(\omega, x) = \overline{a}(x) + \sum_{k=1}^{\infty} \sqrt{\lambda_k}\phi_k(x)\xi_k(\omega),$$

where $\{(\lambda_k, \phi_k)\}_{k\geq 1}$ is the eigenset of the (self-adjoint) covariance operator and $\{\xi_k \sim N(0, 1)\}_{k\geq 1}$ are i.i.d. random variables. It turns out in many cases that it holds that $\lambda_k = O(\ell^r)$ for some $r > 1$ depending on the spatial domain D where the PDE is defined (cf. Chapter 7 of [19]). Consequently, for a medium with small correlation length ℓ, we can write

$$a(\omega, x) = \overline{a}(x) + \sqrt{\lambda_1}\zeta(x, \omega), \qquad \zeta(x, \omega) := \sum_{k=1}^{\infty} \sqrt{\frac{\lambda_k}{\lambda_1}}\, \phi_k(x)\xi_k(\omega),$$

Thus, setting $\varepsilon = \sqrt{\lambda_1} = O(\ell^{\frac{r}{2}})$ gives rise to $a(\omega, x) = \overline{a} + \varepsilon\zeta$, which is the desired "weak form" consisting of a deterministic field plus a small random perturbation. Therefore, our multimodes Monte Carlo finite-element method can still be applied to such random elliptic PDEs in more general form.

It should be pointed out that the classical Karhunen-Loève expansion may be replaced by other types of expansion formulas which may result in more efficient multimodes Monte Carlo methods. The feasibility and competitiveness of non-Karhunen-Loève expansion techniques will be investigated in a forthcoming paper, where comparison among different expansion choices will also be studied. Finally, we remark that the finite element method can be replaced by

any other space discretization method such as finite difference, discontinuous Galerkin, and spectral methods in the main algorithm.

ACKNOWLEDGMENTS

The research of the first author was partially supported by the NSF grant DMS-1318486 and the research of the second author was supported by the NSF grant DMS-1417676. The authors would like to thank the anonymous referee for the valuable suggestions which help to improve the presentation of the paper.

REFERENCES

1. Babuška, I., Nobile, F., and Tempone, R., A stochastic collocation method for elliptic partial differential equations with random input data, *SIAM Rev.*, 52:317–355, 2010.
2. Babuška, I., Tempone, R., and Zouraris, G. E., Galerkin finite element approximations of stochastic elliptic partial differential equations, *SIAM J. Numer. Anal.*, 42:800–825, 2004.
3. Caflisch, R., Monte Carlo and quasi-Monte Carlo methods, *Acta Numer.*, 7:1–49, 2005.
4. Fouque, J., Garnier, J., Papanicolaou, G., and Solna, K., *Wave Propagation and Time Reversal in Randomly Layered Media*, Vol. 56, Stochastic Modeling and Applied Probability, Springer Science & Business Media, New York, pp. 9–597, 2007.
5. Ishimaru, A., *Wave Propagation and Scattering in Random Media*, IEEE Press, New York, pp. 147–243, 1997.
6. Roman, L. and Sarkis, M., Stochastic Galerkin method for elliptic SPDEs: A white noise approach, *Discrete Contin. Dyn. Syst.*, 6:941–955, 2006.
7. Babuška, I., Tempone, R., and Zouraris, G. E., Solving elliptic boundary value problems with uncertain coefficients by the finite element method: the stochastic formulation, *Comput. Methods Appl. Mech. Eng.*, 194:1251–1294, 2005.
8. Deb, M., Babuška, I., and Oden J., Solution of stochastic partial differential equations using Galerkin finite element techniques, *Comput. Methods Appl. Mech. Eng.*, 190:6359–6372, 2001.
9. Eiermann, M., Ernst, O., and Ullmann, E., Computational aspects of the stochastic finite element method, *Comput. Vis. Sci.*, 10:3–15, 2007.
10. Liu, K. and Rivière, B., Discontinuous Galerkin methods for elliptic partial differential equations with random coefficients, *Int. J. Comput. Math.*, 90:2477–2490, 2013.
11. Xiu, D. and Karniadakis, G., The Wiener-Askey polynomial chaos for stochastic differential equations, *SIAM J. Sci. Comput.*, 24:619–644, 2002.
12. Xiu, D. and Karniadakis, G., Modeling uncertainty in steady state diffusion problems via generalized polynomial chaos, *Comput. Methods Appl. Mech. Eng.*, 191:4927–4948, 2002.
13. Feng, X., Lin, J., and Lorton, C., An efficient numerical method for acoustic wave scattering in random media, *SIAM/ASA J. Uncertainty Quantif.*, 3:790–822, 2015.
14. Adams, R. and Fournier, J. J., *Sobolev Spaces*, 2nd ed., Vol. 140, Pure and Applied Mathematics, Elsevier, Oxford, pp. 23–78, 2003.
15. Gilbarg, D. and Trudinger, N. S., *Elliptic Partial Differential Equations of Second Order*, Classics in Mathematics, Springer-Verlag, Berlin, pp. 144–218, 2001.
16. Lions, J. L. and Magenes, E., *Non-Homogeneous Boundary Value Problems and Applications*, Springer-Verlag, New York, pp. 109–226, 1972.
17. Brenner, S. and Scott, L., *The Mathematical Theory of Finite Element Methods*, Vol. 15, Texts in Applied Mathematics, Springer Science & Business Media, New York, pp. 129–151, 2008.
18. Duerinckx, M., Gloria, A., and Otto, F., *The Structure of Fluctuations in Stochastic Homogenization*, [March 15, 2016 from https://arxiv.org/abs/1602.01717], Mar. 9, 2016.
19. Lord, G., Powell, C. and Shardlow, T., *An Introduction to Computational Stochastic PDEs*, Cambridge University Press, New York, pp. 257–309, 2014.